Analytical Methods

PAPER

Check for updates

Cite this: *Anal. Methods*, 2019, **11**, 4651

Determination of phenol degradation in chloride ion rich water by ferrate using a chromatographic method in combination with on-line mass spectrometry analysis†

Debo Wu,[ab] Yihan Xiong,[b] Minghe He,[c] Shuiping Yang,*[a] Jialing Cai,[a] Zhangxiong Wu,[b] Shengpeng Sun,[b] Xiaodong Chen[b] and Winston Duo Wu*[b]

Received 18th July 2019
Accepted 21st August 2019

DOI: 10.1039/c9ay01527b

rsc.li/methods

The degradation of phenol in Cl^--rich water by Fe(VI) was investigated using both chromatographic methods (HPLC and IC) and an on-line direct mass spectrometry (MS) analysis technique. Participation of Cl^- during phenol degradation was observed through the formation of *p*-chlorophenol and coupled species with phenol. Though only a small concentration of Cl^- was involved in the reaction, the presence of Cl^- could affect the behavior of phenol substantially. With the increase of the Cl^- concentration, generation of *p*-benzoquinone and *p*-chlorophenol was increased. Meanwhile, phenol in the bulk solution displayed a sharp decline followed by a gradual increase. The developed on-line MS analysis facilitated real-time monitoring of phenol changes in the reaction system. The results showed that phenol degradation by Fe(VI) with the presence of a high concentration of Cl^- followed a second-order reaction process. The degradation pathway of phenol was also identified, with *p*-chlorophenol, *p*-benzoquinone, maleic acid and formic acid as the main byproducts.

1 Introduction

As one of the common organic pollutants, phenolic compounds are listed as priority pollutants by the United States Environmental Protection Agency (USEPA). A high concentration of phenol and its derivatives has caused severe environmental problems due to their toxicity and persistence in the environment.[1] To date, many techniques have been investigated to solve the problem, including physical adsorption, chemical coagulation and biological treatment.[2–5] However, some of these methods still exhibit limitations and drawbacks. Chemical treatments, such as chlorination and ozonation, have been widely used for phenol removal. However, chlorination may result in the formation of chlorinated phenols and non-biodegradable byproducts. Ozonation may cause the formation of carcinogenic bromate in bromide rich media.[6] In addition, the presence of a high concentration of Cl^- in aquatic environments further increases the complexity of efficient removal of phenolic contaminants. Previous studies have shown that the presence of a high concentration of Cl^- had a significantly inhibitory effect on degradation of organic compounds when using microbial treatment, due to the fact that high salinity could lower the effectiveness of aerobic and anaerobic microorganisms by disrupting microbial growth. Fenton treatment and ozone catalytic oxidation are based on *in situ* generation of highly reactive hydroxyl radicals ($^{\bullet}OH$). However, a previous study showed that the presence of Cl^- could potentially decrease the degradation efficiency of organic contaminants by capturing reactive $^{\bullet}OH$.[7]

The tetra-oxy iron(VI) compound of ferrate (Fe(VI)) is thought to be a sustainable green oxidant due to its high oxidation ability and disinfection properties in a single dose. Fe(VI) is a powerful oxidizing agent throughout the entire pH range, from 2.20 V in acidic environments to 0.72 V in basic environments. The reactions between Fe(VI) and contaminants mainly occur through (i) generation of Fe(V) or Fe(IV) through 1-e^- or 2-e^- transfer and (ii) further reactions of Fe(V) or Fe(IV) with contaminants.[8] The decomposition of Fe(VI), Fe(V) and Fe(IV) results in the formation of Fe(III), an efficient coagulant for heavy metals and phosphate.[9,10] Fe(VI) has been studied for treatment of a variety of organic contaminants[11–16] and a minor range of heavy metals.[17–19] Pilot-scale drinking water treatment using Fe(VI) has been evaluated with a dosage of 0.1 mg L^{-1},

[a]*Jiangxi Key Laboratory for Mass Spectrometry and Instrumentation, East China University of Technology, Nanchang 330013, P. R. China. E-mail: wxipysp@163.com; Fax: +86-791-8389-6370; Tel: +86-791-8389-6370*

[b]*Suzhou Key Laboratory of Green Chemical Engineering, School of Chemical and Environmental Engineering, College of Chemistry, Chemical Engineering and Materials Science, Soochow University, Suzhou, Jiangsu, 215123, P. R. China. E-mail: duo.wu@suda.edu.cn; Fax: +86-512-6588-2750; Tel: +86-512-6588-2762*

[c]*Koovine Environmental Protection Technology, Kunshan, Suzhou, Jiangsu, 215300, P. R. China*

† Electronic supplementary information (ESI) available. See DOI: 10.1039/c9ay01527b

without further pH neutralization. The results showed that, in comparison with ozonation and $FeCl_3$ coagulation, Fe(VI) could not only remove metformin, benzotriazole, and acesulfame from raw water, but also avoid the formation of bromate.[20]

However, though Fe(VI) could potentially be used for removal of phenol and some metal(loid)s, the degradation mechanism of phenol or phenolic compounds with the presence of a high concentration of Cl^- has only scarcely been reported.[21,22] Conventional analytical methods normally require tedious manipulation procedures, including sampling, quenching, preservation, dilution and so on. Also, the determination of various analytes may be easily influenced by complex matrices. Therefore, robust analytical methods which enable sensitive analysis of various analytes without tedious sample preparation are urgently necessary. Extractive electrospray ionization (EESI) is a novel and representative ionization technique for direct and sensitive analysis of various components, such as human breath,[23] native proteins[24] and radioactive elements.[25] In EESI, a spray of charged droplets is formed by infusing a solvent mixture into a conventional ESI source. Another sprayer was used to nebulize the sample solution. Collision between charged droplets and sample aerosol particles occurred and the analytes were then efficiently extracted. Therefore, EESI can tolerate highly complex matrices and can be directly applied under ambient conditions. Based on this, the objectives of the present study were to (1) develop an on-line EESI-MS method for monitoring phenol degradation; (2) evaluate the influence of Cl^- on phenol removal.

2 Experimental

2.1 Materials

All reagents used were of analytical grade, and all solutions were prepared with double deionized (DDI) water obtained from a Millipore water purification system (MilliQ Advantage A10, 18 MΩ cm). Phenol (≥99%, Aladdin), *p*-benzoquinone (≥99%, Adamas), *p*-chlorophenol (≥99%, Adamas), formic acid (99%, Energy), maleic acid (≥99%, for HPLC, Macklin), oxalic acid (99%, Aladdin), succinic acid (99.5%, Aladdin), catechol (99.5%, Macklin), hydroquinone (99.5%, Macklin), acetic acid (≥99.7%, Aladdin) and methanol (99.9%, for HPLC, Sigma-Aldrich) were dissolved in water to obtain their stock solutions (1000 mg L^{-1}). These stock solutions were kept at 4 °C in the dark. Standards of lower concentrations were prepared daily by appropriate dilution with water. Potassium ferrate (K_2FeO_4) with high purity (95%) was prepared in the laboratory by a previously reported method.[26]

2.2 Experimental procedure

Batch experiments were conducted in a 250 mL conical flask containing 100 mL of a mixed solution (0.1 mM phenol and 0.05 M Cl^-). The flask was placed in a thermostatic shaker bath (20 °C) with a rotation speed of 400 rpm at atmospheric pressure. Aliquots of the reaction solution were periodically taken from the container on a predetermined time scale, and the samples were immediately adjusted to a pH of 2.0 with phosphoric acid to quench the further reaction between Fe(VI) and phenol. To study the influence of Cl^- on phenol degradation, a series of mixed solutions containing 0.1 mM phenol and various concentrations of Cl^- (from 0 to 0.5 M) were prepared and then reacted with Fe(VI) at pHs of 6.5 and 9.0. All experiments were conducted in triplicate. All samples were filtered using a syringe filter with a pore size of 0.25 μm. On-line analysis of phenol degradation was carried out using extractive electrospray ionization mass spectrometry (EESI-MS), as illustrated in Fig. 1.

2.3 Analytical methods

The concentrations of phenol, *p*-benzoquinone, catechol and *p*-chlorophenol were measured by high-performance liquid chromatography (HPLC, Agilent 1260) coupled with diode array detection (DAD). Chromatographic separation was performed using an Eclipse Plus C18 column (3.5 μm, 4.6 × 100 mm). A mixture of methanol and water (50 : 50, v/v) with a flow rate of 0.5 mL min^{-1} was used as the eluent. Phenol, *p*-benzoquinone, catechol and *p*-chlorophenol, detected at wavelengths of 270, 245, 275 and 227 nm, were eluted out at 4.4, 2.8, 3.0 and 9.7 min, respectively. The detection limits for phenol, *p*-benzoquinone, catechol and *p*-chlorophenol were 0.05, 0.05, 0.1 and 0.08 mg L^{-1}, respectively. The concentrations of Cl^-, formic acid and maleic acid were detected on an ion chromatograph (IC, ICS600, Thermo Fisher), equipped with an AS23 anion exchange column. A combination of Na_2CO_3 (4.5 mM) and $NaHCO_3$ (0.8 mM) was used as the mobile phase, with a flow rate of 1.0 mL min^{-1}. Dissolved organic carbon during phenol removal was determined using a total organic carbon analyzer (TOC, Shimadzu TOC-L CPH).

The setup of the on-line MS detection device is shown in Fig. 1. A 50 mL round bottom flask was used as the reactor and was loaded with the phenol and Cl^- mixture (0.1 mol L^{-1} phenol and 0.125 mol L^{-1} Cl^-). A gas flowmeter (0.15–1.5 L min^{-1}) (Changzhou Edkorx Instrument co., LTD.) and a glass rotameter (LZB-3WB) were used to adjust the flow of the carrier gas (N_2) (0.3 MPa, 0.8 L min^{-1}). The gas pressure for the electrospray was 1.0 MPa, also with N_2 as the carrier gas. Generally, N_2 was introduced into the reaction vessel through glass tubes. A PEEK tube was used to transport the analytes to the mass spectrometer. After introduction of N_2, bubbles were continuously generated in the flask. A micro spray was then formed by the fine droplets resulting from bubble bursting,[27,28] exactly reflecting the components of the bulk solution. The formed

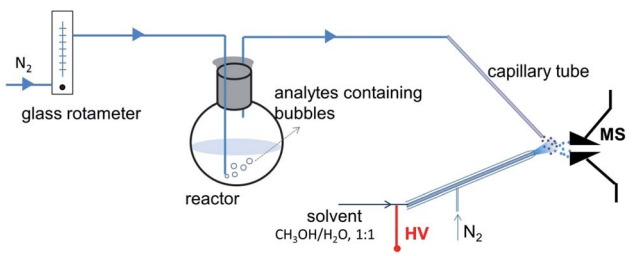

Fig. 1 The experimental setup of on-line EESI-MS for real-time monitoring of phenol degradation.

This journal is © The Royal Society of Chemistry 2019

micro spray then interacted with the droplets of the electrospray solvent (methanol and water mixture). The angle between the two sprayers of the EESI instrument was about 38°, and the tips of the sprayers were about 5 mm away from the inlet capillary of the mass spectrometer. An LTQ-XL linear ion trap spectrometer (Finnigan, San Jose, CA) was used as the detector for on line analysis. Negative ion detection mode was used. The ionization voltage was set at −4.5 kV accordingly, and the capillary temperature was set at 350 °C. Mass spectra were recorded in the mass range of *m*/*z* 25–200 with a maximum ion injection time of 100 ms. Collision induced dissociation (CID) experiments were performed by applying 30% collision energy for 30 ms to the precursor ions. Other parameters were set by default for LTQ-MS.

3 Results and discussion

3.1 Intermediates produced during phenol degradation

Although the toxicity and carcinogenicity have been widely identified, the degradation mechanism of phenol is still disputable, probably due to the fact that the degradation intermediates and pathways varied significantly depending on reaction conditions,[29–31] *e.g.* pH, oxidants and matrices. In addition, the lack of robust analytical methods which allow efficient chromatographic separation and accurate detection of intermediate products at trace levels also posed a great challenge to further investigation. In this study, chromatographic methods (HPLC and IC) in combination with an on-line direct MS technique were used to investigate the mechanism of phenol removal in Cl^- rich water samples. Chromatographic methods were developed for measurement of possible byproducts like *p*-chlorophenol, *p*-benzoquinone, hydroquinone, catechol, formate, maleic acid, oxalate, succinic acid and acetic acid. These byproducts were then identified by comparing their elution times with those of the standards (Fig. S1 and S2†). The results were then compared with those of on-line MS analysis.

At a pH of 9, with an Fe(VI) : phenol molar ratio of 5 : 1, four byproducts were successfully quantified: *p*-chlorophenol, *p*-benzoquinone, and formic and maleic acids (Fig. 2). *p*-Chlorophenol and *p*-benzoquinone emerged in the beginning of reaction and then decreased gradually with increasing reaction time and eventually disappeared. The ring-opening products maleic acid and formic acid were detected as well, which subsequently reached equilibrium and remained constant in solution. The concentrations of both phenol and TOC decreased as a function of reaction time, indicating partial mineralization of the parent compound. In addition, trace levels of catechol, succinic acid and oxalic acid were also observed by HPLC or ion chromatography (Fig. S3 and S4†); however their peaks were too weak for accurate quantification (see the ESI†). With an Fe(VI) : phenol molar ratio of up to 20 : 1, neither *p*-benzoquinone nor *p*-chlorophenol was detected, probably due to the even faster reaction between Fe(VI) and phenol. Under these conditions, the formed formic acid and maleic acid, however, were significantly elevated (by 4.1 mg L^{-1} and 3.1 mg L^{-1}, respectively) (Fig. S5†). Generally, *p*-benzoquinone was the main intermediate during phenol degradation,[29,32] and maleic acid and formic acid were the main ring-cleavage products.[33]

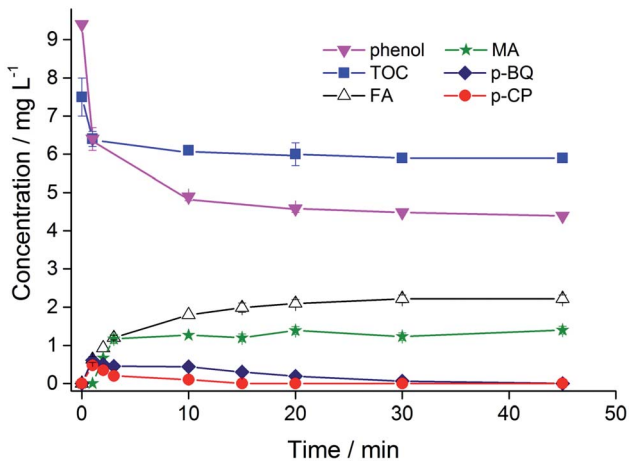

Fig. 2 Concentration evolution of *p*-benzoquinone (*p*-BQ), *p*-chlorophenol (*p*-CP), maleic acid (MA), formic acid (FA) and residual phenol, along with the solution TOC. [phenol] = 0.1 mM, [Cl^-] = 0.05 M, Fe(VI) : phenol (molar ratio) = 5 : 1, pH = 9.0.

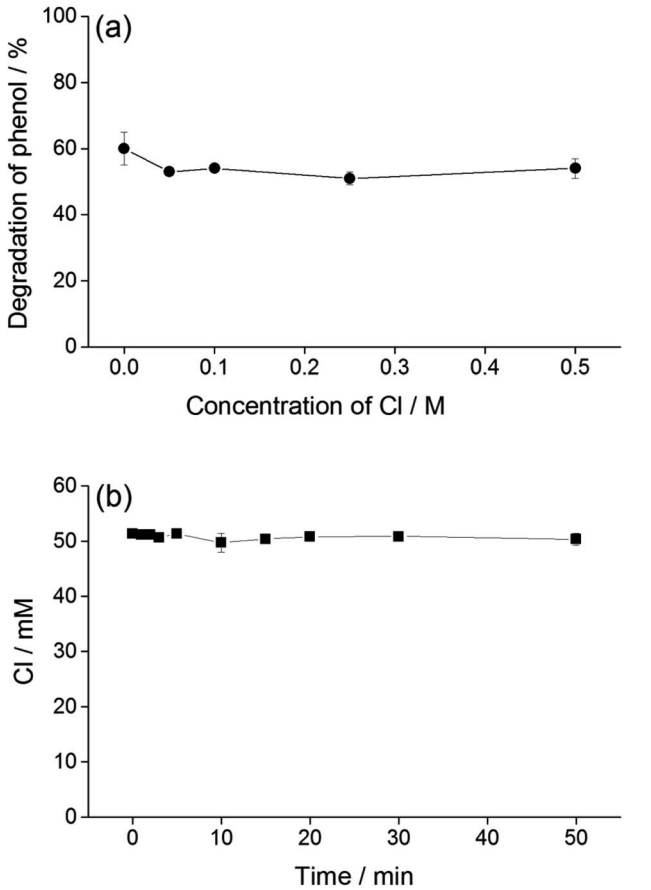

Fig. 3 (a) Degradation of phenol as a function of Cl^- concentration (0.0–0.5 M); (b) the behavior of Cl^- (0.05 M) during the phenol degradation process. [phenol] = 0.1 mM, Fe(VI) : phenol (molar ratio) = 10 : 1, pH = 9.0.

3.2 Influence of co-existing Cl^- on phenol degradation

The removal of phenol as a function of Cl^- concentration and the behavior of Cl^- during phenol removal are shown in Fig. 3(a) and (b). Generally, phenol removal remained more or less stable with increasing concentrations of Cl^- from 0 to 0.5 M. Continuous monitoring of Cl^- on a time scale of 50 min also suggested that Cl^- generally remained constant (0.05 M) during the whole removal process. This was in agreement with a previous study that Cl^- impurities resulting from the synthesis of sulfatoferrate(VI) had no obvious negative impact on phenol removal and mineralization by sulfatoferrate(VI).[29] However, in our study, a small concentration of *p*-chlorophenol (<0.5 mg L^{-1}) was detected at 1 min, and it subsequently decreased gradually (Fig. 2), indicating that participation of Cl^- during phenol removal did occur. Therefore, the behavior of Cl^- was further investigated by measuring produced *p*-chlorophenol at different Cl^- concentrations under neutral conditions. It can be seen in Fig. 4 that residual phenol in solution after removal generally increased slightly with the increase of Cl^- from 0 to 0.25 M. These results indicated that the removal percentage of phenol with the presence of a high Cl^- concentration was relatively lower than that with a low Cl^- concentration, probably due to the fact that higher Cl^- concentrations resulted in more production of *p*-chlorophenol which could not facilitate the degradation of phenol. Without Cl^-, phenol in solution showed a sharp decline followed by a mild decrease. Considering that the reaction between phenol and Fe(VI) was a rapid process, the sharp decline was ascribed to degradation by Fe(VI), which accounted for about 89% of removed phenol. On the other hand, the mild decrease (about 11% of removed phenol) was probably due to adsorption by the formed precipitate, since decomposition of Fe(VI) could result in the production of Fe(III) which was able to sequester various contaminants by forming Fe(III)-(oxy)hydroxide. With elevated Cl^- concentrations (*e.g.* Cl^- = 0.25 M), however, phenol in solution was regenerated partially after an even stronger drop, which was probably due to the formation of a reversible state of phenol, *e.g.* dimers or trimers, since a previous study has revealed that a substantial amount of radical coupled products for phenol could be formed during oxidation by Fe(VI).[21] On the other hand, the yields of *p*-benzoquinone and *p*-chlorophenol were also elevated with the increasing Cl^- concentration. The behaviors of phenol, *p*-benzoquinone and *p*-chlorophenol suggested that a higher concentration of Cl^- in water could promote the formation of *p*-benzoquinone and *p*-chlorophenol during phenol degradation by Fe(VI). Although only a small concentration of Cl^- was involved, it could influence the behavior of phenol notably during degradation by Fe(VI).

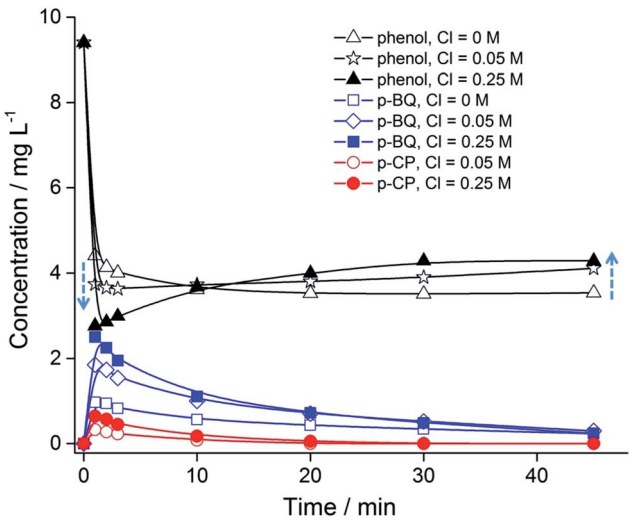

Fig. 4 Behaviors of *p*-chlorophenol (*p*-CP), *p*-benzoquinone (*p*-BQ) and residual phenol in solutions with different Cl^- concentrations during the phenol degradation process. [phenol] = 0.1 mM, Fe(VI) : phenol (molar ratio) = 5 : 1, pH = 6.5.

3.3 On-line analysis of phenol degradation with direct mass spectrometry analysis

It can be seen in Fig. 2 that phenol degradation by ferrate was a rapid process. Therefore, tedious conventional analytical methods were not adequate to evaluate the degradation

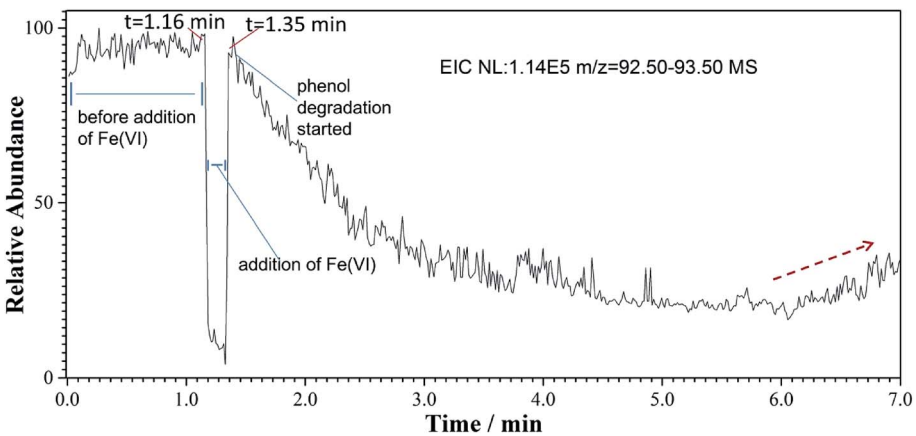

Fig. 5 EIC of phenol (m/z = 93) obtained by on-line EESI-MS. The EIC of phenol for t = 0–1.16 min before addition of Fe(VI) and t = 1.16–1.37 min for the duration of Fe(VI) addition. [phenol] = 0.1 M, [Cl^-] = 0.25 M, Fe(VI) = 0.5 M, pH = 6.5.

This journal is © The Royal Society of Chemistry 2019

behavior of phenol, particularly the study of its reaction kinetics. Based on this, an on-line analysis device was built to help monitor the reaction using an ambient mass spectrometry technique which allowed direct analysis of various analytes without sample preparation.[34,35] As a representative newly emerging ambient mass spectrometry analysis technique, EESI-MS has the advantages of high sensitivity, fast analysis and avoidance of matrix influences.[24,25,36–38] Therefore, it is ideal for real-time monitoring of the phenol degradation process without being influenced by extremely high concentrations of chloride. The EESI instrument has two separate sprayers, one to nebulize the sample solution and the other to produce charged micro-droplets of the solvent (Fig. 1). The reactants and intermediates generated during phenol degradation were carried to the MS inlet and sprayed out of a capillary using N_2(g). The analytes were then extracted using solvent microdroplets for further MS analysis (Fig. 1). It can be seen from the extracted ion chromatograms (EICs) of phenol (Fig. 5) that, before addition of Fe(VI) (0–1.16 min), only a high abundance of phenol (m/z 93) could be observed as deprotonated $[M–H]^-$ (Fig. S6†). The stable signal intensity of m/z 93 indicated stable formation of the micro spray and efficient ionization of analytes. Phenol

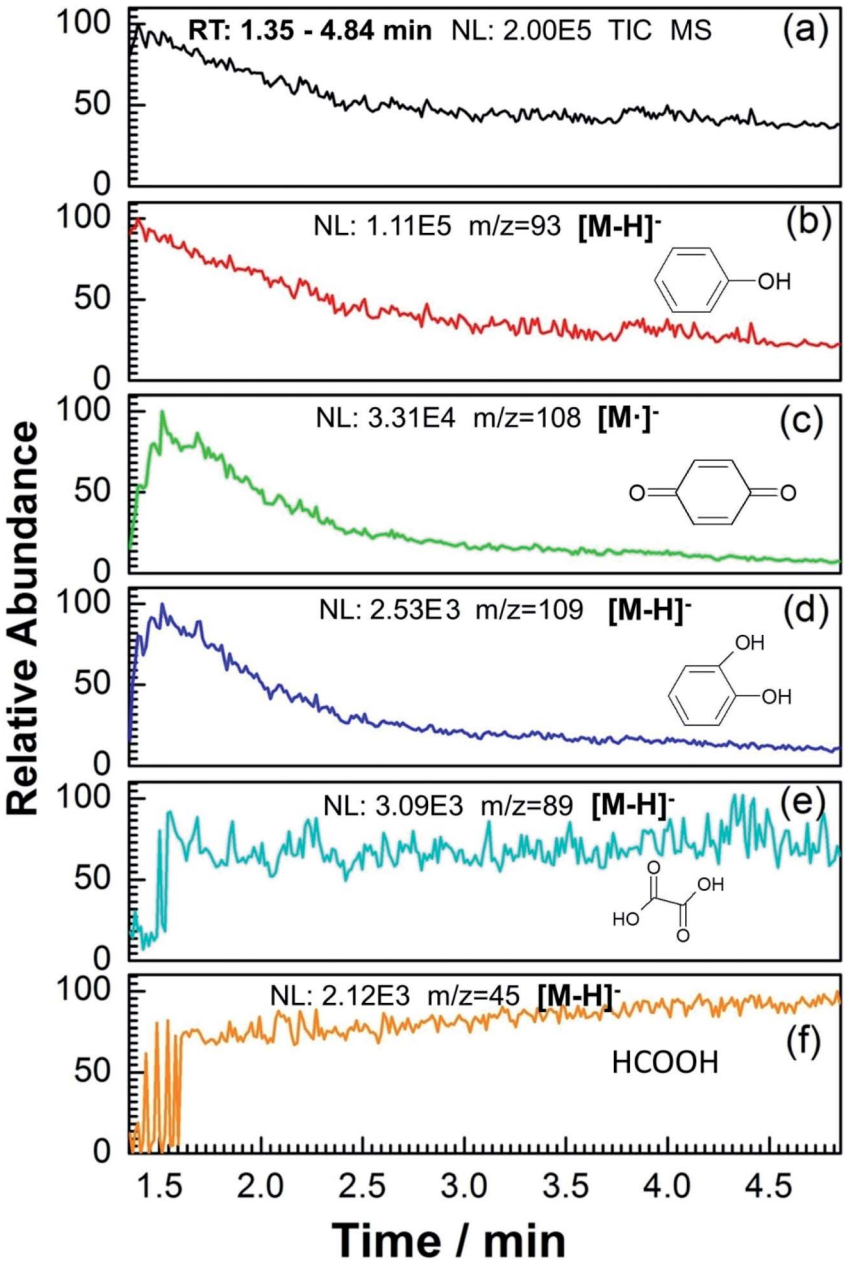

Fig. 6 EICs of phenol (m/z = 93) and typical intermediates obtained by on-line EESI-MS. Data were collected in the time duration of 1.35–4.84 min. (a) Total ion chromatography (TIC); (b)–(f) the extracted ion chromatograms of phenol ($[M–H]^-$, m/z = 93), p-benzoquinone ($[M^{\bullet}]^-$, m/z = 108), catechol ($[M–H]^-$, m/z = 109), oxalic acid ($[M–H]^-$, m/z = 89) and formic acid ($[M–H]^-$, m/z = 45). [phenol] = 0.1 M, $[Cl^-]$ = 0.25 M, Fe(VI) = 0.5 M, pH = 6.5.

degradation was then initiated by addition of Fe(VI) (t = 1.35 min). The relative abundance of phenol then decreased gradually as a function of reaction time. It is worth noting that from 6.0 min onwards, the intensity of phenol showed an increasing tendency (Fig. 5), which was in agreement with the off-line HPLC analysis that residual phenol in solution displayed a drastic decrease followed by a gradual increase in Cl^- rich media. On the other hand, immediately after phenol degradation started, significant peak intensities at m/z 108 and 109 were observed (Fig. 6 and S7†). After about 4 min of the reaction, the peaks at m/z 108 and 109 decreased obviously, and an enhancement of m/z 89 and m/z 45 was observed (Fig. 6 and S8†). Further CID analysis showed that molecular ions at m/z 108 generated fragmentation ions of m/z 80 due to loss of CO (Fig. S9†), while those at m/z 109 generated fragmentation ions of m/z 81 and 91 due to loss of CO and H_2O, respectively (Fig. S10†). This indicated that the molecular ions at m/z 108 and 109 were *p*-benzoquinone and catechol. In addition, it can be seen in the EICs (Fig. 6) of various analytes that each component behaved similarly to those in previous offline analysis, *e.g.* phenol generally showed a gradual decrease in the first few minutes, and *p*-benzoquinone increased sharply and then decreased gradually in solution. Generation of oxalic acid and formic acid was also observed. Noteworthily, in addition to the above observed peaks such as m/z 89 and m/z 108, a notable peak at m/z 219 was also detected (Fig. 7). CID analysis showed that m/z 219 generated fragment peaks at m/z 203, 191 and 163, due to loss of O, 2O and 2CO fragments, respectively. Further CID analysis suggested that fragmentation ions of m/z 203 generated m/z 187 by losing O fragments. Consequently, the peak at m/z 219 was concluded to be the combination of phenol and *p*-chlorophenol as shown in Fig. 7. The temporary formation of coupled products during the reaction may well explain the reason why with the presence of higher concentrations of Cl^-, phenol demonstrated an even stronger decline followed by a subsequent gradual increase.

On the other hand, direct on-line MS analysis also facilitated the study of the reaction kinetics of phenol degradation. By studying the extracted ion chromatogram of phenol, the concentration changes of phenol as a function of reaction time could be obtained (Fig. 5 and 6), and therefore the kinetics of phenol degradation could be evaluated. Fig. 8 shows the kinetic fitting of phenol degradation with the data obtained from the EIC of phenol within 5 min from the point when phenol degradation was initiated. It can be seen that $1/C$ (phenol, L mg^{-1}) was linearly correlated with t (min), indicated by the high correlation coefficient ($R^2 = 0.916$) (Fig. 8). These results suggest that phenol degradation in Cl^- rich media by ferrate could be expressed as $1/C_{phenol} - 1/C_{phenol,0} = kt$, and therefore it fits the second-order reaction process.

3.4 Degradation pathway of phenol in Cl^--rich media

Previous spin-trapping analysis and electron paramagnetic resonance (EPR) spectroscopy has showed that phenol was degraded by Fe(VI) through a radical reaction pathway, involving the formation of phenoxyl radicals in the first step.[32] Therefore, the degradation pathway of phenol by Fe(VI) in Cl^--rich media could be proposed as follows (Fig. 9): (1) reactive phenoxy radicals (together with another two resonance structures of 2-hydroxyphenyl and 4-hydroxyphenyl radicals) and Fe(V) were formed *via* 1-e^- transfer; (2) phenoxy radicals continued to react with Fe(V) to form *p*-benzoquinone and Fe(III), which was a 2-e^- oxidation process; (3) *p*-benzoquinone was further decomposed into maleic acid and a trace amount of succinic acid through ring cleavage; (4) maleic acid was oxidized to formic acid and further to carbon dioxide. Meanwhile, succinic acid was decomposed to oxalic acid. On the other hand, a small concentration of chlorine free radicals were generated due to

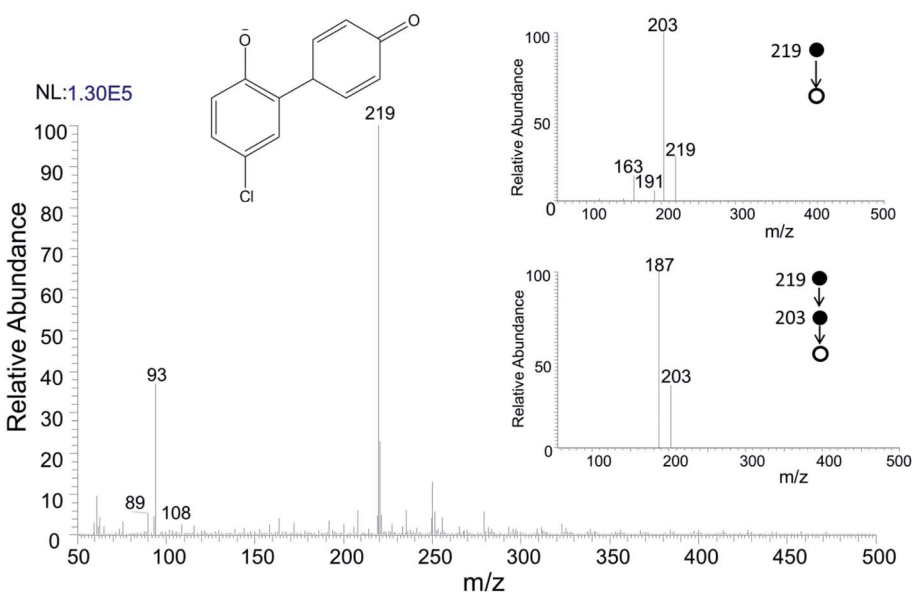

Fig. 7 The MS spectrum of m/z 219 obtained during phenol degradation by Fe(VI) using on-line EESI-MS.

 This journal is © The Royal Society of Chemistry 2019

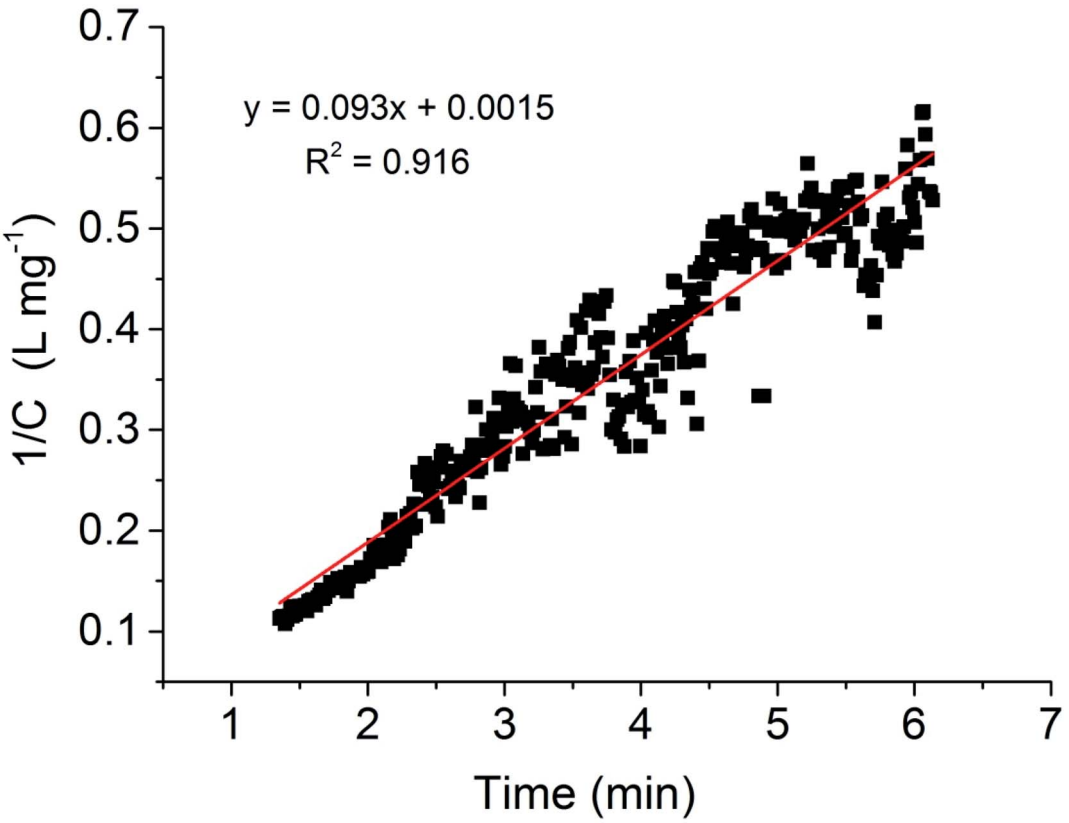

Fig. 8 Kinetics of phenol degradation by Fe(VI). Data were obtained by online EESI-MS analysis in the time range between $t = 1.35$ min (the point when phenol degradation was initiated) and $t = 6$ min.

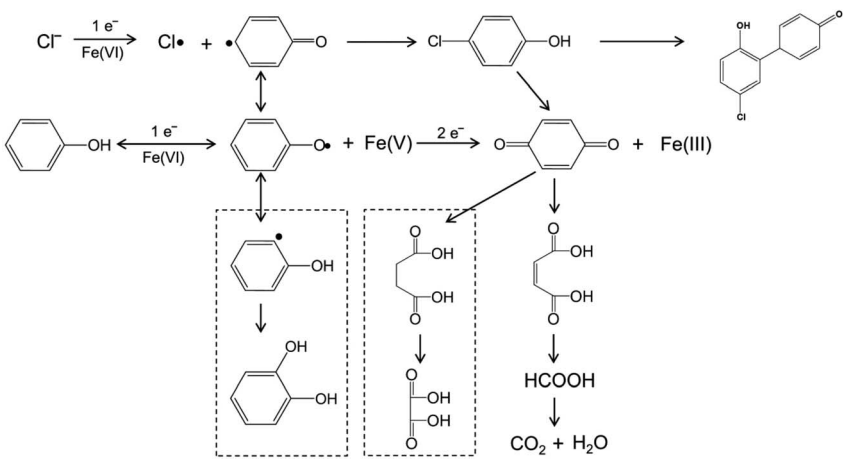

Fig. 9 Pathway of phenol degradation with the presence of a high concentration of Cl^- by Fe(VI).

the action of Fe(VI) on Cl^-, which then reacted with 4-hydroxyphenyl radicals to form *p*-chlorophenol[29] and further *p*-benzoquinone. A combined species between phenol and *p*-chlorophenol was also formed *via* radical coupling. In addition, a small concentration of 2-hydroxyphenyl radicals, resulting from the reaction between phenol and Fe(VI) as well, were converted into catechol. Clearly, phenol was mainly degraded by forming *p*-benzoquinone and subsequently maleic acid and formic acid. The presence of a high concentration of Cl^- had a promoting effect on *p*-benzoquinone and *p*-chlorophenol production.

4 Conclusions

In this study, phenol degradation in a Cl^--rich aquatic environment by Fe(VI) was investigated using conventional

chromatographic analytical methods (HPLC and IC) in combination with an on-line direct mass spectrometry technique. Chromatographic methods enabled quantification of various components, while the on-line MS technique has the advantage of real-time monitoring of reactants and intermediates without being influenced by high concentrations of Cl^-. Our study demonstrated that Fe(VI), as a green water treatment reagent, could potentially be applied for efficient removal of phenol even with the presence of a high concentration of Cl^-. Participation of Cl^- could significantly alter the behavior of phenol during the degradation process; however it displayed a minor effect on the final removal percentage of phenol. The degradation pathway of phenol in Cl^--rich media by Fe(VI) was also identified, with *p*-chlorophenol, *p*-chlorophenol–phenol coupled species, *p*-benzoquinone, maleic acid and formic acid as the main byproducts.

Conflicts of interest

There are no conflicts to declare.

Acknowledgements

This work was supported by project funding from the Natural Science Foundation of China (Grant No. 21506135), the Natural Science Foundation of Jiangsu Province (No. BK20140317), and the Priority Academic Program Development (PAPD) of Jiangsu Higher Education Institutions. Xiao Dong Chen and Zhangxiong Wu acknowledge the start-up grant from Soochow University.

References

1 L. Gianfreda, G. Iamarino, R. Scelza and M. A. Rao, *Biocatal. Biotransform.*, 2006, **24**, 177–187.
2 L. Yu, X. Wu, Q. Liu, L. Liu, X. Jiang, J. Yu, C. Feng and M. Zhong, *J. Nanosci. Nanotechnol.*, 2016, **16**, 12426–12432.
3 X. Wei, H. Wu, G. He and Y. Guan, *J. Hazard. Mater.*, 2017, **321**, 408–416.
4 R. S. Juang and C. Y. Wu, *Chemosphere*, 2007, **66**, 191–198.
5 B. Li, K. Sun, Y. Guo, J. Tian, Y. Xue and D. Sun, *Fuel*, 2013, **110**, 99–106.
6 U. Von Gunten, *Water Res.*, 2003, **37**, 1469–1487.
7 R. Maciel, G. L. Sant'Anna and M. Dezotti, *Chemosphere*, 2004, **57**, 711–719.
8 V. K. Sharma, R. Zboril and R. S. Varma, *Acc. Chem. Res.*, 2015, **48**, 182–191.
9 R. Prucek, J. Tuček, J. Kolařík, I. Hušková, J. Filip, R. S. Varma, V. K. Sharma and R. Zbořil, *Environ. Sci. Technol.*, 2015, **49**, 2319–2327.
10 R. P. Kralchevska, R. Prucek, J. Kolařík, J. Tuček, L. Machala, J. Filip, V. K. Sharma and R. Zbořil, *Water Res.*, 2016, **103**, 83–91.
11 B. Yang, R. S. Kookana, M. Williams, G.-G. Ying, J. Du, H. Doan and A. Kumar, *J. Hazard. Mater.*, 2016, **320**, 296–303.
12 W. Gan, V. K. Sharma, X. Zhang, L. Yang and X. Yang, *J. Hazard. Mater.*, 2015, **292**, 197–204.
13 M. Feng, L. Cizmas, Z. Wang and V. K. Sharma, *Chemosphere*, 2017, **177**, 144–148.
14 M. Feng, L. Cizmas, Z. Wang and V. K. Sharma, *Chem. Eng. J.*, 2017, **323**, 584–591.
15 K. Manoli, G. Nakhla, M. Feng, V. K. Sharma and A. K. Ray, *Chem. Eng. J.*, 2017, **330**, 987–994.
16 X. Sun, K. Zu, H. Liang, L. Sun, L. Zhang, C. Wang and V. K. Sharma, *J. Hazard. Mater.*, 2018, **344**, 1155–1164.
17 S. A. Baig, T. Sheng, Y. Hu, J. Xu and X. Xu, *Clean: Soil, Air, Water*, 2015, **43**, 13–26.
18 M. D. Johnson and B. B. Lorenz, *Sep. Sci. Technol.*, 2015, **50**, 1611–1615.
19 Y. Lee, I. H. Um and J. Yoon, *Environ. Sci. Technol.*, 2003, **37**, 5750–5756.
20 J.-Q. Jiang, H. B. P. Durai, M. Petri, T. Grummt and R. Winzenbacher, *Desalin. Water Treat.*, 2016, **57**, 26369–26375.
21 J. Chen, N. Wu, X. Xu, R. Qu, C. Li, X. Pan, Z. Wei and Z. Wang, *Environ. Sci. Technol.*, 2018, **52**, 12592–12601.
22 J. Chen, X. Xu, X. Zeng, M. Feng, R. Qu, Z. Wang, N. Nesnas and V. K. Sharma, *Water Res.*, 2018, **143**, 1–9.
23 H. Chen, A. Wortmann, W. Zhang and R. Zenobi, *Angew. Chem., Int. Ed.*, 2007, **46**, 580–583.
24 H. Chen, S. Yang, M. Li, B. Hu, J. Li and J. Wang, *Angew. Chem., Int. Ed.*, 2010, **49**, 3053–3056.
25 M. Luo, B. Hu, X. Zhang, D. Peng, H. Chen, L. Zhang and Y. Huan, *Anal. Chem.*, 2010, **82**, 282–289.
26 C. Li, X. Z. Li and N. Graham, *Chemosphere*, 2005, **61**, 537–543.
27 K. Chingin, Y. Cai, V. Chagovets, A. Kononikhin, N. Starodubtseva, V. Frankevich and H. Chen, *Metabolomics*, 2016, **12**, 1–8.
28 K. Chingin, Y. Cai, J. Liang and H. Chen, *Anal. Chem.*, 2016, **88**, 5033–5036.
29 T. Pigot and V. Peings, *J. Environ. Manage.*, 2015, **157**, 287–296.
30 C. Li, X. Z. Li, N. Graham and N. Y. Gao, *Water Res.*, 2008, **42**, 109–120.
31 D. Amado-Piña, G. Roa-Morales, C. Barrera-Díaz, P. Balderas-Hernandez, R. Romero, E. Martín del Campo and R. Natividad, *Fuel*, 2017, **198**, 82–90.
32 H. Huang, D. Sommerfeld, B. C. Dunn, E. M. Eyring and C. R. Lloyd, *J. Phys. Chem. A*, 2001, **105**, 3536–3541.
33 X. Xie, Y. Hu and H. Cheng, *Water Res.*, 2016, **89**, 59–67.
34 J. Han, W. Liu, R. Su, L. Zhu, D. Wu, J. Xu, A. Liu, H. Zhang, W. Kou, X. Zhang and S. Yang, *Anal. Bioanal. Chem.*, 2019, **411**, 3281–3290.
35 M. Rahman, D. Wu and K. Chingin, *J. Am. Soc. Mass Spectrom.*, 2019, **30**, 814–823.
36 C. Liu, B. Hu, J. Shi, J. Li, X. Zhang and H. Chen, *J. Anal. At. Spectrom.*, 2011, **26**, 2045–2051.
37 H. Chen, A. Venter and R. G. Cooks, *Chem. Commun.*, 2006, 2042–2044.
38 L. Zhu, G. Gamez, H. Chen, K. Chingin and R. Zenobi, *Chem. Commun.*, 2009, 559–561.

 This journal is © The Royal Society of Chemistry 2019